Titre: Title:	Multi–Dimensional Wireless Signal Identification Based on Support Vector Machines
Auteurs: Authors:	Kürşat Tekbıyık, Özkan Akbunar, Ali Riza Ekti, Ali Görçin, & Gunes Karabulut Kurt
Date:	2019
Type:	Article de revue / Article
Référence: Citation:	Tekbıyık, K., Akbunar, Ö., Ekti, A. R., Görçin, A., & Karabulut Kurt, G. (2019). Multi–Dimensional Wireless Signal Identification Based on Support Vector Machines. IEEE Access, 7, 138890-138903. https://doi.org/10.1109/access.2019.2942368

IEEE Access
Multidisciplinary : Rapid Review : Open Access Journal

Received August 23, 2019, accepted September 13, 2019, date of publication September 19, 2019, date of current version October 4, 2019.

Digital Object Identifier 10.1109/ACCESS.2019.2942368

Multi–Dimensional Wireless Signal Identification Based on Support Vector Machines

KÜRŞAT TEKBIYIK[1,2], (Student Member, IEEE), ÖZKAN AKBUNAR[1,2], (Student Member, IEEE), ALİ RIZA EKTİ[1,3], (Member, IEEE), ALİ GÖRÇİN[1,4], (Senior Member, IEEE), AND GÜNEŞ KARABULUT KURT[2], (Senior Member, IEEE)

[1]Informatics and Information Security Research Center (BİLGEM), TÜBİTAK, 41470 Kocaeli, Turkey
[2]Department of Electronics and Communications Engineering, İstanbul Technical University, 34467 İstanbul, Turkey
[3]Department of Electrical–Electronics Engineering, Balıkesir University, 10145 Balıkesir, Turkey
[4]Department of Electronics and Communications Engineering, Yıldız Technical University, 34349 İstanbul, Turkey

Corresponding author: Kürşat Tekbiyik (tekbiyik@itu.edu.tr)

ABSTRACT Radio air interface identification provides necessary information for dynamically and efficiently exploiting the wireless radio frequency spectrum. In this study, a general machine learning framework is proposed for Global System for Mobile communications (GSM), Wideband Code Division Multiple Access (WCDMA), and Long Term Evolution (LTE) signal identification by utilizing the outputs of the spectral correlation function (SCF), fast Fourier Transform (FFT), auto–correlation function (ACF), and power spectral density (PSD) as the training inputs for the support vector machines (SVMs). In order to show the robustness and practicality of the proposed method, the performance of the classifier is investigated with respect to different fading channels by using simulation data. Various over–the–air real–world measurements are taken to show that wireless signals can be successfully distinguished from each other without any prior information while accounting for a comprehensive set of parameters such as different kernel types, number of in–phase/quadrature (I/Q) samples, training set size, or signal–to–noise ratio (SNR) values. Furthermore, the performance of the proposed classifier is compared to the existing well–known deep learning (DL) networks. The comparative performance of the proposed method is also quantified by classification confusion matrices and Precision/Recall/F_1–scores. It is shown that the investigated system can be also utilized for spectrum sensing and its performance is also compared with that of cyclostationary feature detection spectrum sensing.

INDEX TERMS Cyclostationarity, FFT, machine learning, power spectral density, spectral correlation function, spectrum sensing, support vector machine, wireless signal identification.

I. INTRODUCTION

Wireless communications systems are currently witnessing a fascinating growth in the volume of data transmissions, device diversity, number of devices and networks. Thus, limited spectrum resources can hardly meet the dynamically changing and ever–increasing demands of 5G and beyond wireless mobile networks [1]. Many researchers investigate to carry out a multi–disciplinary effort including the deployment of small cells, employment of mmWave communications, efficient spectrum usage algorithms, device-to-device (D2D) communications and massive multiple–input multiple–output (MIMO) systems [2], as well as cognitive radio networks, to cope up with these demands. Among them, authorities such as the Federal Communications Commission (FCC) and researchers put a specific emphasis on improving the performance of spectrum sensing as well as signal recognition algorithms to provide a better and more reliable quality of service (QoS) levels while considering the wide variety of device diversity, network topology, transmission schemes and channel conditions. However, contemplating all these metrics within a single framework can only be achieved by utilizing

The associate editor coordinating the review of this manuscript and approving it for publication was Jon Atli Benediktsson.

intelligent functions such as machine learning methods across the wireless infrastructure and end–user devices. Within this framework, it is expected that smart communication devices will identify and detect the radio frequency (RF) signals, which are deployed in many commercial and tactical fields to select the most appropriate transmission schemes.

Wireless signal identification has been employed in various military and civilian communication systems, such as electronic warfare, radio surveillance and spectrum awareness. In the past, classical signal identification tasks heavily relied on complex collections of feature extraction methods such as higher order cumulants and complex hierarchical based decision trees. In addition, classical signal processing approaches are vulnerable to false alarms and modifications are required over them when a new technology emerges. Therefore, data–centric machine learning–based methods, which incorporate the imperfections and real–world effects will produce a more robust, efficient and resilient performance compared to the classical methods.

A. RELATED WORK

Signal identification techniques mainly utilize likelihood based (LB) and feature based (FB) identification techniques. The LB approaches maximize the probability of correct classification. However, LB methods have high computational complexity and are sensitive to model mismatches such as timing offsets and channel coefficients estimations [3]–[5].

In FB approaches, various features which are extracted from signals are employed for the detection of the type of incoming signals. Features such as the wavelet transform, higher order statistics and cyclic features are present in the literature for signal identification problems. Along this line, instantaneous amplitude, phase and frequency statistics are utilized to classify the modulation types of signals in [6], [7]. In [8], [9], phase shift keying (PSK) and frequency shift keying (FSK) signals are identified via wavelet transform. Another feature is higher order statistics such as higher order moments and cumulants which are used for signal classification in [10]–[12]. However, these features are more sensitive to real–world conditions such as timing and frequency offsets.

The most powerful FB approach for signal identification in real–world conditions makes use of cyclostationarity based–features because these features are robust to model mismatches [13]. Accordingly, PSK, FSK and quadrature amplitude modulation (QAM) signals are distinguished by using features obtained with cyclostationary signal processing [14], [15]. In addition to modulation classification, cyclostationary signal identification is employed in the identification of radio interfaces such as Global System for Mobile communications (GSM), Wideband Code Division Multiple Access (WCDMA), Long Term Evolution (LTE), and worldwide interoperability for microwave access (WiMAX). In [16], it has been shown that second–order cyclostationarity can be used for the classification of LTE and GSM signals. Cyclic patterns of three air interfaces, which are GSM, code division multiple access (CDMA), and orthogonal frequency division multiplexing (OFDM), are investigated in [17] and constant false alarm rate (CFAR) test is employed to detect the features. Moreover, to identify IEEE 802.11 signals, the authors use second–order cyclostationarity [18]. In [19], second–order cyclostationarity due to cyclic prefix, preamble and reference signals are employed to identify LTE and WiMAX signals. Except cyclostationarity–based identification, the performance of the aforementioned approaches degrades due to real–world wireless conditions such as fading, path loss, and time shift.

Machine learning and deep learning (DL)–based identification methods have been recently used in signal classification due to the rapid development in this area. Convolutional neural network (CNN), convolutional long short term memory fully connected deep neural network (CLDNN) and long short term memory (LSTM) are the most popular deep neural network architectures for signal identification. In [20], spectral correlation function (SCF) is fed into a neural network for the generic signals amplitude modulation (AM), PSK, and FSK. In [21], the various modulation schemes are classified by using SCF and support vector machine (SVM). To identify radar signals, CNN is utilized in [22]. CNN is also employed for interference identification in wireless communications [23]. In [24], CNNs with the fast Fourier Transform (FFT), in–phase/quadrature (I/Q) data and amplitude–phase representations are used for modulation identification and interference identification in industrial, scientific and medical (ISM) band. In [25], the authors utilize LSTM to identify digital video broadcasting (DVB), Radar, terrestrial trunked radio (TETRA), LTE, GSM and wide-Band FM (WFM) via FFT, I/Q data, and amplitude–phase representation. Besides DL, SVM is used in the signal identification problems due to the fact that SVM based classifier can be implemented on field programmable gate array [26], [27], which makes it a good choice for practical applications. Wu *et al.* propose a modulation recognition system including SVM and higher order cumulants in [28]. By choosing features robust to noise, the system does not require to train for each signal–to–noise ratio (SNR) value. In [29], SVM is employed to identify modulation types in the presence of channel impairments. Recently, it is shown that SVM outperforms in the classifier set consisting different models for the automatic modulation classification in cooperative relaying networks [30]. Besides modulation classification, [31] proposes an SVM–based approach to jointly estimate modulation and the SNR. Our previous work [32] indicates the classification performance of SVM with SCF. However, there was no parametric analysis to observe the classifier performance with regard to the parameters of the classification system.

B. CONTRIBUTIONS

The survey above indicates the growing literature on the use of SVMs for modulation recognition. When the literature in this domain is investigated, it is seen that currently there is no comprehensive and inclusive work on the investigation of implementation of SVM–based identifiers for air interface identification as the signals are transmitted in a multiplexed manner when compared to the directly modulated signals. Thus, this work utilizes SVMs for air interface identification. Even though in this study the focus is on cellular signals, the proposed framework can be applied to any air interface since each signal should have to carry some distinctive features inherently to make the communications possible. Therefore, the proposed framework incorporates the processed outputs of cellular signals, which are comprised of such inherent features with SVMs for signal identification. Since the SVMs learn these features directly from the processed outputs, statistical decision mechanisms that are utilized by classical identifiers are immediately eliminated. Furthermore, it is shown that identification procedures that are based on SVMs have a superior performance than that of classical detection and estimation techniques depending on the statistical inference mechanisms. The main contributions of this study are summarized as follows:

- A conceptual framework for blind wireless signal identification is proposed, which is followed by detailed description of the methodology for collecting spectrum data, designing wireless signal representations, forming training data and utilizing SVM for wireless signal classification. To demonstrate the proposed approach, an SVM–based wireless standard–based signal identification method is proposed by utilizing the FFT, auto–correlation function (ACF), power spectral density (PSD), and SCF as the features for SVM. This eliminates the need for a two step identification approach of classical sensing techniques. The performance of the proposed method is also compared to the classical sensing technique of cyclostationary feature analysis.
- A comprehensive set of wireless signal identification features such as FFT, ACF, PSD, and SCF are provided on this interdisciplinary topic along with their comparison for wireless standard based signal identification. Three well–known and mostly available wireless signal types are analyzed: GSM, WCDMA and LTE. We also share the over–the–air signal measurements dataset in the format of FFT, ACF, PSD, and α–domain profile by maximizing SCFs over spectral frequency; thus, it can be directly fed into any classifier [33].
- In–depth parametric analysis is performed to show the impact of the performance and accuracy of the wireless signal classifier by examining different features, kernels, received signal lengths, training set sizes, and fading types in the presence of additive white Gaussian noise (AWGN). Most of the signal identification researches overlook the effect of wireless environment conditions and assume AWGN channel [34]–[36]. However, in this study, we propose a blind signal identification system by using over–the–air signal measurements of the new dataset (i.e. real propagation effects). To account for the signal imperfections present in the nature of real–world conditions (e.g. fading, multipath, and so on), we propose a SVM based classifier system which is robust to dynamic nature of the wireless signal propagation environment. The proposed system is also compared to existing well–known DL algorithms such as CLDNN and LSTM.

C. ORGANIZATION OF THE PAPER

The rest of this paper is organized as follows: In Section II, the signal model is provided. In Section III, we present the features used with SVMs. Section IV details the mathematical preliminaries of the SVMs. Data collection and processing are given in Section V. Results and discussions are presented in Section VI and conclusions are drawn in Section VII. Also, the glossary list is provided in Appendix.

II. SIGNAL MODEL

The complex baseband equivalent of the received signal, $r(t)$, in a fading environment with noise is given as

$$r(t) = x(t) * \rho(t) + \omega(t), \tag{1}$$

where $\omega(t)$ denotes a sample function of the AWGN process with a flat power spectral density $N_0/2$ W/Hz; $x(t)$ is the complex baseband equivalent of the unknown signal; $\rho(t)$ stands for the impulse response for the time–varying wireless channel; and $*$ denotes the convolution operator. Consequently, the problem can be defined as identifying the unknown signal $x(t)$ using cyclostationary signal processing to obtain the discriminating characteristics of $r(t)$ in the presence of AWGN and multipath fading without any apriori knowledge for any of them.

III. FEATURES

In this section, we detail four different features extracted from the received signals and used to identify the type of cellular communication through the proposed classification. The features utilized are named as SCF, FFT, ACF, and PSD.

A. SPECTRAL CORRELATION FUNCTION

Cyclostationary signal processing is used to extract the hidden periodicities within the received signal, $r(t)$ [14]. The hidden periodicities show unique characteristics for different cellular communication signals in terms of symbol periods, spreading codes, guard intervals, and even message bits. As a result, cyclostationary signal processing can extract features from the received signals to discriminate them.

In this study, the second–order cyclostationarity of signals is investigated by taking the non–linear transformation as

$$s_\tau(t) = \mathbb{E}\left\{r(t+\tau/2)r^*(t-\tau/2)\right\}, \tag{2}$$

where $s_\tau(t)$ is the auto–correlation of $r(t)$. As widely known the auto–correlation function is periodic with T_0 for second–order cyclostationary signals [37]. Therefore, it can be expanded to Fourier series coefficients as

$$\mathcal{R}_r^\alpha(\tau) = \frac{1}{T_0}\int_{-T_0/2}^{T_0/2} s_\tau(t)\exp\left(-j2\pi\alpha t\right)dt. \tag{3}$$

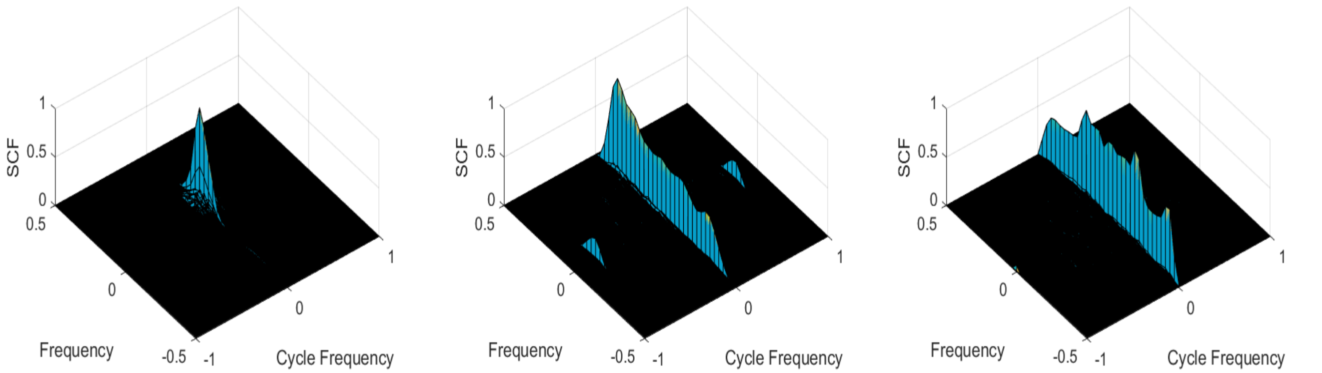

(a) GSM (b) WCDMA (c) LTE

FIGURE 1. **SCFs estimated by FAM algorithm in bi–frequency plane after mapping for various cellular communication signals.**

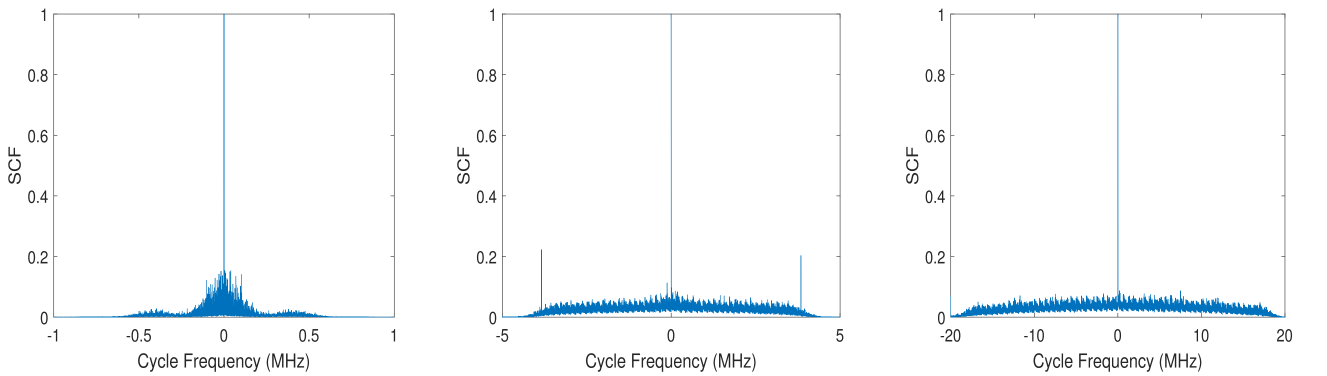

(a) GSM (b) WCDMA (c) LTE

FIGURE 2. **α–domain profiles evaluated by maximizing SCFs over spectral frequency.**

$\mathcal{R}_r^{\alpha}(\tau)$ is known as the cyclic auto–correlation function (CAF), where the cyclic frequency is denoted by α. It is noted that the frequency domain representation of the signals can also provide some distinct characteristics regarding $r(t)$. Then the Fourier transform of CAF for a fixed α can be analyzed by using cyclic Wiener relation [14]

$$\mathcal{S}_r^{\alpha}(f) = \int_{-T/2}^{T/2} \mathcal{R}_r^{\alpha}(\tau) \exp(-j2\pi f\tau)\, d\tau. \quad (4)$$

$\mathcal{S}_r(f)$ is named as SCF and it is obvious that SCF gives the PSD when α is zero.

$$\mathbb{S}_{rT}^{\alpha_i+q\Delta\alpha}\left(nL, f_j\right) = \sum_k R_T\left(kL, f_m\right) R_T^*\left(kL, f_l\right) \cdot g_c(n-k)\, e^{-i2\pi kq/P} \quad (5)$$

The computation of SCF has a very high computational complexity. In order to reduce this complexity, the FAM is used, which is originally proposed in [15], and based on time smoothing via FFT. The SCF corresponding to the received signal, $r(t)$ is estimated by FAM via (5), where $R_T(n,f)$ is complex–valued demodulates which is the N'–point FFT of $r(n)$ passed through a Hamming window, computing with

$$R_T(n,f) = \sum_{k=-N'/2}^{N'/2} a(k) r(n-k) e^{-i2\pi f(n-k)T_s}. \quad (6)$$

In this study, the Hamming window and unit rectangle window are used as data tapering windows in FAM. Hamming window and unit rectangle window are represented with $a(n)$ and $g_c(n)$, respectively in (5) and (6). T_s, N', and L are the sampling period, channelization length and sample size of hopping blocks, respectively. The SCF of wireless communication signals which are estimated via FAM is depicted in Fig. 1.

After bi–frequency mapping, the output matrix of SCF has the dimensions 64 × 16385 when 16384 I/Q samples are used. In order to reduce the size of feature vectors, instead of using the bi–frequency domain of SCF, α–domain profile is employed by evaluating the maximum over spectral frequency such that

$$I(\alpha) = \max_f |\mathcal{S}_r^{\alpha}(f)|. \quad (7)$$

As a result, the feature size decreases to 1 × 16385. For the signals to be classified, the α–domain profiles are depicted

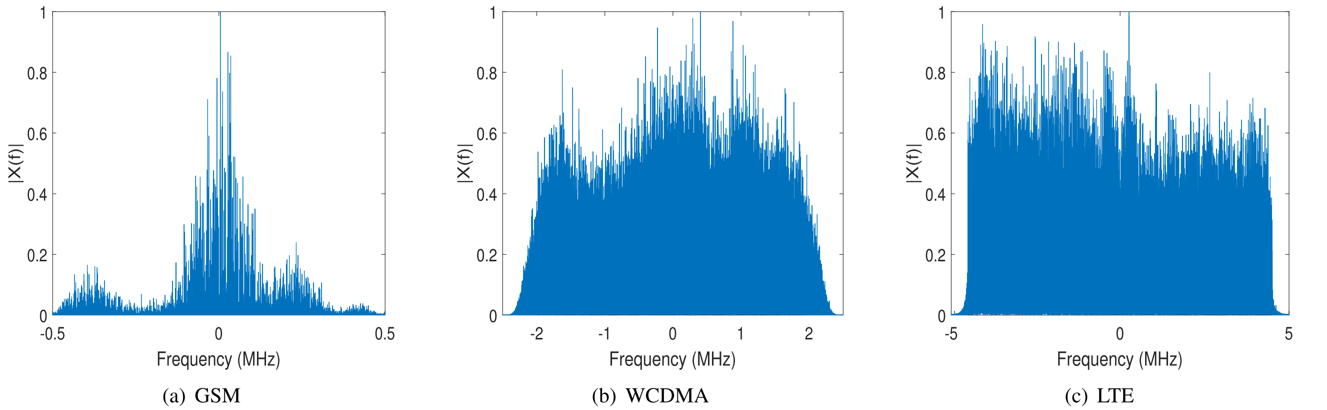

FIGURE 3. FFTs for cellular communication signals.

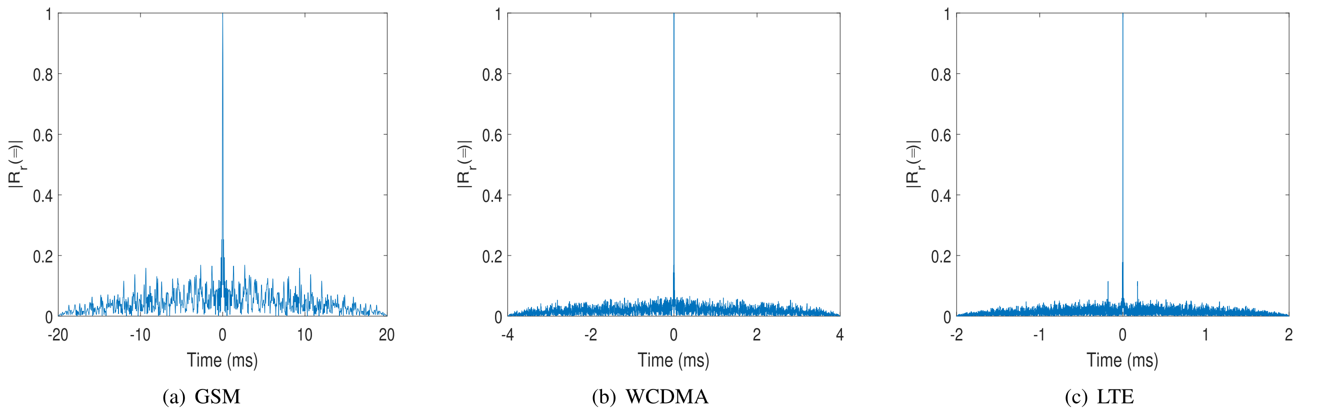

FIGURE 4. ACFs for cellular communication signals.

in Fig. 2. It is easily seen that the α–domain profiles for GSM, WCDMA, and LTE signals show unique characteristics. Therefore, they can be employed as feature vectors for a classifier. The feature vector is constructed as

$$\mathbf{x} = [I(-f_s + \Delta\alpha),\ I(-f_s + 2\Delta\alpha), \cdots,\ I(f_s)]^T, \tag{8}$$

where f_s is the sampling frequency and $\Delta\alpha$ indicates the cyclic resolution. It is employed by SVM as detailed in Section IV.

B. FAST FOURIER TRANSFORM

The frequency domain representation of a signal are employed as a discriminating feature. This is extracted from time domain I/Q data via an FFT operation. FFT is defined as

$$R_k = \sum_{n=0}^{N-1} r[n] e^{-j2\pi kn/N}, \quad k = 1, \ldots, N-1. \tag{9}$$

and $r(n)$ is samples of signal $r(t)$

$$r[n] = r(\frac{t}{f_s}), \quad n = 0, \ldots, N-1. \tag{10}$$

Frequency domain representations of sample GSM, WCDMA and LTE signals are depicted in Fig. 3. The feature vector for FFT is defined as

$$\mathbf{x} = \left[R_0,\ R_1, \cdots, R_{N-1}\right]^T. \tag{11}$$

C. AUTO–CORRELATION FUNCTION

The ACF extracts unique patterns from different cellular communication signals due to periodicities in the time domain. For instance, in the time domain of GSM signals, there exists periodicity due to midambles [38]. This periodic pattern is revealed by the ACF. In addition, due to the usage of cyclic prefix to eliminate inter–symbol interference [39], the periodicity corresponding to cyclic prefixes can also be seen in the ACF of LTE signals. ACF for the cellular communication signals are in Fig. 4. ACF sequence of received waveform is investigated to make a decision about the type of communication signal. ACF of signal is defined as

$$R_r(k) = \sum_{n=0}^{N-1} r[n] r[n-k], \quad k = 0, \ldots, 2N-1. \tag{12}$$

Then, the feature vector is

$$\mathbf{x} = [R_r(0),\ R_r(1), \cdots, R_r(2N-1)]^T. \tag{13}$$

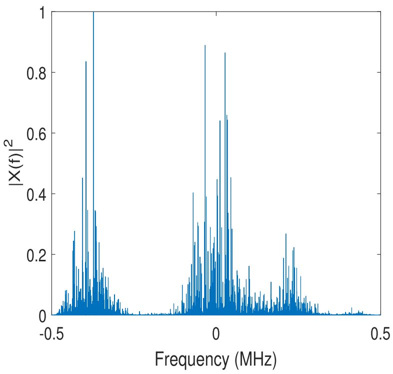

(a) GSM

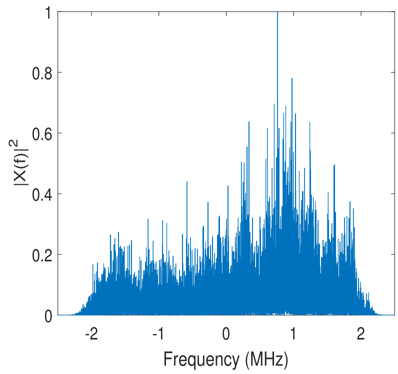

(b) WCDMA

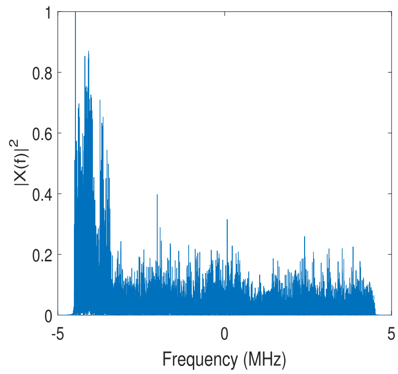

(c) LTE

FIGURE 5. PSDs for cellular communication signals.

D. POWER SPECTRUM DENSITY

The PSD of cellular communication signals can be used as a feature vector in order to differentiate signals because the power spectra are related to the bandwidth and the channel in which the signal propagates through. PSD is the Fourier transform of the ACF and is calculated as follow

$$S_r(f) = \sum_{k=-\infty}^{\infty} R_r(n)e^{-j2/N}, \quad k = 1, \ldots, N-1. \quad (14)$$

PSDs in the linear scale are presented in Fig. 5 for GSM, WCDMA, and LTE signals.

PSD has almost the same characteristics as FFT since

$$|P_r(f)| = |\mathcal{F}\{r(n)\}|^2, \quad (15)$$

where $|\cdot|$ denotes the magnitude. The feature vector obtained from PSD is given as

$$\mathbf{x} = \left[R_0^2,\ R_1^2, \cdots, R_{N-1}^2\right]^T. \quad (16)$$

Especially, in the logarithmic scale, it is expected to show almost same performances.

E. COMPUTATIONAL COMPLEXITY ANALYSIS

Computational complexity is an important parameter for feature selection when considering specifications of a processing unit. Optimal features can be chosen by taking prediction accuracy into consideration as well as its computation time. In regards to the problem, we provide the computational complexity of feature generation for the features used in this study. The computational complexity of SCF estimated by FAM is $\mathcal{O}(2N[4 + 2\log_2(N') + 4N + 2N' + N'\log_2(\frac{4N}{N'})])$, where N is the received signal length [15]. FFT has the computational complexity $\mathcal{O}(N\log_2(N))$. The computational complexity that is the same for both ACF and PSD is $\mathcal{O}(N^2)$. Even though SCF is the most computationally complex feature among them, the training complexity of SVM is reduced by using the α−domain profile of the SCF.

IV. SUPPORT VECTOR MACHINES

SVM is a supervised machine learning method originally used for binary classification. SVMs aim to find the optimal decision boundary referred to as the hyperplane. In essence, this plane is chosen such that the separation between two classes in the feature space is maximized.

Consider a given training dataset $\{(\mathbf{x}_1, y_1), (\mathbf{x}_2, y_2), \cdots, (\mathbf{x}_n, y_n)\}$ with a feature vector $\mathbf{x}_k \in \mathbb{R}^n$ and label $y_k \in \mathbb{R}$ for the k−th signal. Feature vectors described in the previous sections are utilized in an SVM classifier as

$$y_k\left[\omega^T\psi(\mathbf{x}_k) + b\right] \geq 1 - \zeta_k, \quad k = 1, \ldots, n, \quad (17)$$

where ω and b denote the weight vector and the decision bias, respectively. $\psi(\cdot)$ is the transformation applied for the kernel trick as

$$\mathcal{K}(\mathbf{x}_k, \mathbf{x}_l) = \psi(\mathbf{x}_k)^T\psi(\mathbf{x}_l), \quad (18)$$

and ζ is a slack variable for the linearly non–separable case, noting that it is zero for the linearly separable case. The slack variable is employed to tolerate misclassifications [40]. Convex optimization methods are used to maximize the margin between data points and the hyper plane given as

$$\begin{aligned} &\min_{\omega,b,\zeta} \frac{1}{2}\omega^T\omega + c\sum_{k=1}^{n}\zeta_k \\ &\text{such that } y_k\left[\omega^T\psi(\mathbf{x}_k) + b\right] \geq 1 - \zeta_k, \\ &\qquad \zeta_k \geq 0, \quad k = 1, \ldots, n, \end{aligned} \quad (19)$$

where c is a positive real constant. The Lagrangian for the optimization problem given in (19) is expressed as in (20),

$$\mathcal{L}(\omega, b, \zeta; \alpha, \nu) = \frac{1}{2}\omega^T\omega - \sum_{k=1}^{n}\alpha_k\left(y_k\left[\omega^T\psi(\mathbf{x}_k) + b\right] - 1\right) - \sum_{k=1}^{n}\zeta_k(\alpha_k + \nu_k - c) \quad (20)$$

where α_k and ν_k are Lagrange multipliers such that $\alpha_k \geq 0$ and $\nu_k \geq 0$. Using saddle point of the Lagrangian, the dual quadratic programming problem is obtained as follows:

$$\min_{\alpha} \frac{1}{2}\sum_{k=1}^{n}\sum_{l=1}^{n} y_k y_l \mathcal{K}(\mathbf{x}_k, \mathbf{x}_l)\alpha_k \alpha_l - \sum_{k=1}^{n}\alpha_k$$

$$\text{such that } \sum_{k=1}^{n}\alpha_k y_k = 0,$$

$$0 \leq \alpha_k \leq c, \quad k, l = 1, \ldots, n. \tag{21}$$

Then, the SVM classifier can be expressed with the decision function, $f(\mathbf{x})$ such that

$$f(x) = \operatorname{sign}\Big[\sum_{k=1}^{n}\alpha_k y_k \mathcal{K}(\mathbf{x}, \mathbf{x}_k) + b\Big], \tag{22}$$

where $\mathcal{K}(\mathbf{x}, \mathbf{x}_k)$ is the kernel function. Some kernel functions can be defined as

$$\mathcal{K}(\mathbf{x}, \mathbf{x}_k) = \mathbf{x}_k^T \mathbf{x}, \tag{23}$$

$$\mathcal{K}(\mathbf{x}, \mathbf{x}_k) = (\gamma + \mathbf{x}_k^T \mathbf{x})^d, \ \gamma > 0, \tag{24}$$

$$\mathcal{K}(\mathbf{x}, \mathbf{x}_k) = \exp(-|\mathbf{x} - \mathbf{x}_k|_2^2/\sigma^2), \ \sigma \in \mathbb{R} \tag{25}$$

$$\mathcal{K}(\mathbf{x}, \mathbf{x}_k) = \tanh(\kappa_1 \mathbf{x}_k^T \mathbf{x} + \kappa_2) \tag{26}$$

for linear, d–degree polynomial, radial basis function (RBF), and multi–layer perceptron (MLP) kernels, respectively.

The performance metrics mainly used for SVM classifier models are prediction, recall, and F_1–score. These performance metrics give an insight into the characteristics of a designed classifier model. The prediction accuracy is the measure of how well accurate recognition can be performed by an SVM signal classifier. The prediction is given as

$$\Theta = \frac{1}{N_{test}}\sum_{i=1}^{N_{test}} l(\hat{r}_i, r_i), \tag{27}$$

where $\hat{r}_i$ and r_i are the predicted and received signals at any instance i, respectively. Then, $l(\hat{r}_i, r_i)$ takes a value of 1 when the predicted and true signals match, or a 0 value, otherwise. The precision gives a metric of how much the results determined as positive are actually positive. The recall is a measure denoting how much true positives are identified correctly. The harmonic average of precision and recall is named as the F_1–score which is an overall measure for the accuracy of the classifier model. The precision (P), recall (R), and F_1–score are given as

$$P = \frac{\xi}{\xi + \upsilon}, \quad R = \frac{\xi}{\xi + \mu},$$

$$F_1\text{–score} = 2 \times \frac{P \times R}{P + R}, \tag{28}$$

where the number of true positive, false positive, and false negative are denoted by ξ, υ, and μ, respectively.

V. DATASET

The wireless mobile communication dataset used in this study includes GSM, WCDMA and LTE signals which have been received over–the–air from different base stations with unique conditions in terms of the number of taps, fading, and SNR. To illustrate the dataset, the power spectrum estimation by the Welch's method is depicted in Fig. 6.

For the sake of clarity, we emphasize that all signals are received from different channels and at different times. Furthermore, as [41] allows transmissions in the different bandwidths, the dataset includes LTE signals of various bandwidths. The training set and the test set contain 1000 and 500 signals for each waveform, respectively. Each signal is composed of 20000 I/Q samples. We share the dataset in the format of FFT, ACF, PSD, and α–domain profile by maximizing SCFs over spectral frequency; thus, it can be directly fed into any classifier [33].

VI. CLASSIFICATION PERFORMANCE ANALYSIS

Performance of the proposed SVM–based signal classifier is analyzed in terms of the different features, kernels, numbers of I/Q samples, and SNR levels. Unless otherwise stated, SCF, linear, and 16384 are used as optimum parameters for the feature vector, kernel, and the number of I/Q samples, respectively. For these default parameters, 5–fold cross validation gives a mean accuracy of 98% with 1% variance.

A. FEATURE SELECTION

Four feature types are employed individually for the classification of GSM, WCDMA, and LTE signals in the real–world conditions. As described in Section III, FFT, ACF, PSD and SCF are employed, which can give the unique features for the signals owing to their periodicity arising from mid–amble, chip rate, symbol duration, and so on. For instance, FFT creates features associated with spectrum masks defined in the standardization of cellular communication signals. Also, the ACF of GSM signals gives mid–amble position. Another example of ACF leads to peaks with the period related to symbol duration for LTE signals. On the other hand, SCF reveals the hidden periodicities within the signals. To illustrate, the SCF of WCDMA signal takes peak value in α–domain at 3.84 Mcps which is the chip rate for the system operating in 5 MHz bandwidth [42].

When FFT is employed as a feature vector as described in Section III-B, the average accuracy is quite poor such that it almost resembles random selection. The second feature is PSD and the performance of PSD is quite similar to FFT performance because of similar characteristic of operations to FFT. ACF feature shows performance over 74%. Additionally, SCF performs with the accuracy exceeding 95%. The classification results indicate that SCF can be used as a superior feature to identify cellular communication signals in real–world conditions compared to the FFT, PSD and ACF. Furthermore, the feature fusion method is actually used by concatenating four feature vectors which are FFT, PSD, ACF, and SCF. This new vector is fed into SVM. However, one should note that the training and feature extraction processes increase complexity. Then, the results for both feature fusion method and SCF only method are given in Table 1. The results show that SCF only case gives better performance compared to the fusion method, since the diversity of the feature fusion

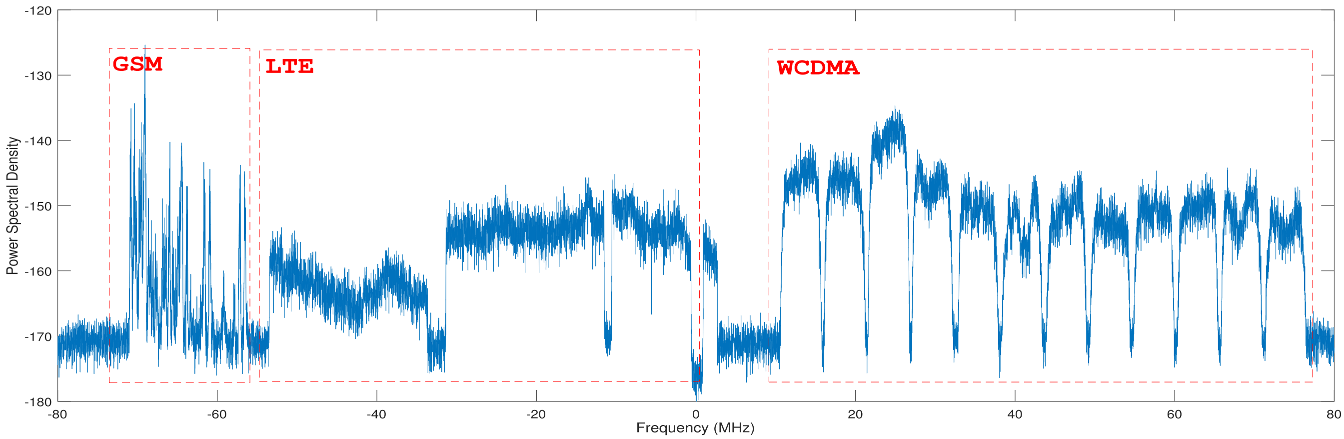

FIGURE 6. The power spectral densities estimated by Welch's method for sample signals in the dataset.

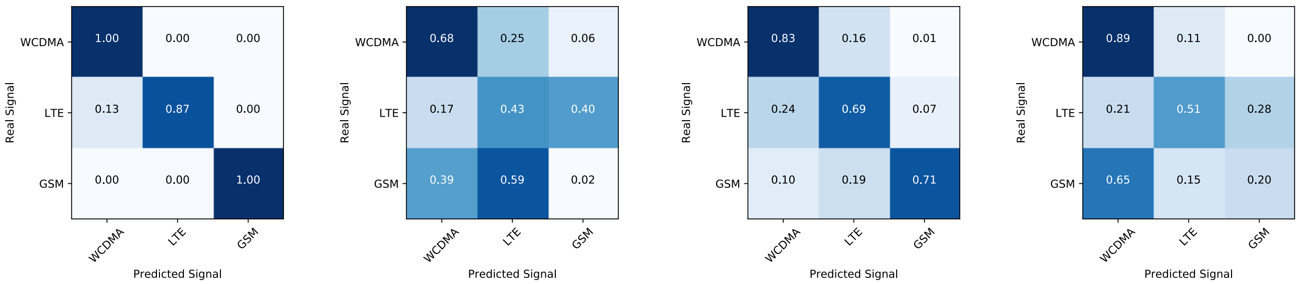

(a) SCF (b) FFT (c) ACF (d) PSD

FIGURE 7. The confusion matrices when the different features used in SVM signal classifier.

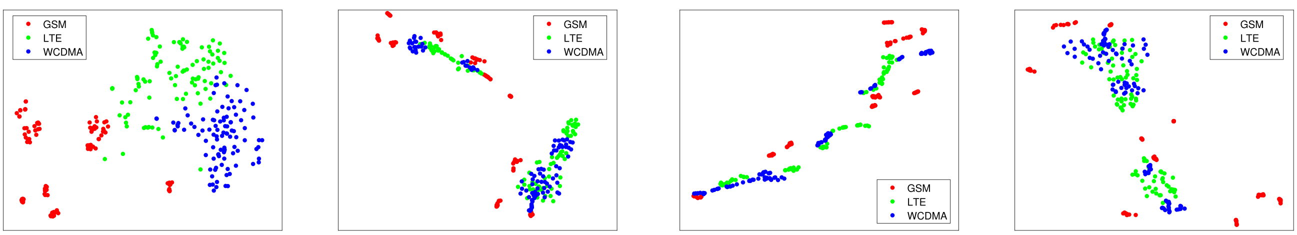

(a) SCF (b) FFT (c) ACF (d) PSD

FIGURE 8. Two–dimensional demonstration of the features by the t–SNE algorithm.

output vector increase drastically. Thus, the feature fusion method provides a bit worse performance results than the SCF only case. The confusion matrices for the classification results are given in Fig. 7. The precision, recall, and F_1–scores are summarized in Table 1.

Moreover, t–distributed stochastic neighbor embedding (t-SNE) algorithm is employed to visualize feature vectors created by SCF, FFT, ACF, and PSD in two–dimensional space. As seen in Fig. 8, SCF outputs feature vectors which are linearly separable. However, other functions are not able to produce linearly separable feature vectors. The results of t-SNE algorithm show why FFT, ACF, and PSD have poor classification performance.

Notably, when the logarithm of features in base ten is employed, the classification accuracy becomes higher. FFT feature with logarithm identifies signals by the ratio of 89%. Likewise, the performance of PSD increases to 89% by taking the logarithm due to the fact that the logarithm of the FFT is equal to the logarithm of the PSD scaled by 2 as aforementioned in Section III-D. At the same time, the logarithm operation also increases the performance of ACF feature from 74% to 93%. In contrast with these features, there is a slight decrease in SCF. This phenomenon is due to the fact that the logarithmic process huddles scattered features in space. By comparing the confusion matrices depicted in Fig. 9 with the matrices given for features without logarithm, it can be

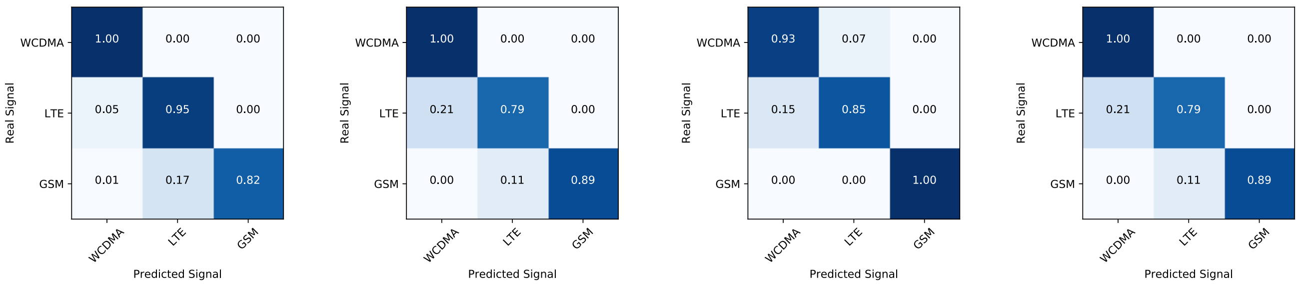

(a) SCF (b) FFT (c) ACF (d) PSD

FIGURE 9. The confusion matrices when the different features with logarithm are used in SVM signal classifier.

TABLE 1. Performance metrics when FFT, ACF, and SCF are individually employed as feature vector in SVM.

Feature	Signal	Precision	Recall	F_1–score
FFT	WCDMA	0.55	0.68	0.61
	LTE	0.34	0.43	0.38
	GSM	0.04	0.02	0.02
	Average	0.31	0.38	0.34
ACF	WCDMA	0.71	0.83	0.76
	LTE	0.66	0.69	0.68
	GSM	0.91	0.71	0.80
	Average	0.76	0.74	0.75
PSD	WCDMA	0.51	0.89	0.65
	LTE	0.66	0.51	0.58
	GSM	0.42	0.20	0.27
	Average	0.53	0.53	0.50
SCF	WCDMA	0.88	1.00	0.94
	LTE	1.00	0.87	0.93
	GSM	1.00	1.00	1.00
	Average	0.96	0.96	0.96
Fusion	WCDMA	0.83	1.00	0.90
	LTE	0.95	0.79	0.86
	GSM	1.00	0.96	0.98
	Average	0.93	0.92	0.92

seen that the logarithm function improves the performance. The performance metrics are listed in Table 2 for the logarithm of features.

SCF performs with a high accuracy in the fading environment at the cost of increased computational complexity. Although FFT, PSD, and ACF show relatively poor classification performances, they have lower computational complexity. By taking the logarithm, these features can be used in SVMs for the classification of signals received in the real–world conditions.

B. SUPPORT VECTOR MACHINE KERNEL TYPE

In this study, the effect of the kernel type of SVM on classification accuracy is investigated. During the performance analysis, 16384 I/Q samples for each candidate signal are utilized as a constant parameter. The training and test sets consist of 1000 and 500 signals for each waveform, respectively. SCF of the received signal is used as a discriminating feature. The results in regards to kernel selection are given in Table 3. Table 3 shows that the linear kernel given with (23) gains an advantage over the others. The linear kernel results with the accuracy of 93%. Besides the performance, the linear kernel

TABLE 2. Performance metrics when the logarithms of FFT, ACF, and SCF are individually employed as feature vector in SVM.

Feature	Signal	Precision	Recall	F_1–score
FFT	WCDMA	0.83	1.00	0.90
	LTE	0.88	0.79	0.83
	GSM	1.00	0.89	0.94
	Average	0.90	0.89	0.89
ACF	WCDMA	0.86	0.93	0.90
	LTE	0.93	0.85	0.89
	GSM	1.00	1.00	1.00
	Average	0.93	0.93	0.93
PSD	WCDMA	0.83	1.00	0.90
	LTE	0.88	0.79	0.83
	GSM	1.00	0.89	0.94
	Average	0.90	0.89	0.89
SCF	WCDMA	0.94	1.00	0.97
	LTE	0.84	0.95	0.89
	GSM	1.00	0.82	0.90
	Average	0.93	0.92	0.92

is faster and simpler in terms of training and classification. Even though the quadratic and polynomial kernels with the degree of three show acceptable performance in a fading environment, MLP and RBF kernels degrade classification performances. The MLP kernel achieves best performance when the weight κ_1 and the bias κ_2 are chosen as 1 and -1, respectively. Especially RBF kernel is noneffective for the recognition of cellular communication signals by using SCF. Nevertheless, σ value is chosen as 10^{-2}, 1, 10, and 100, there is no change in the classification behavior of SVM. It is possible to say that the SVM classifier with RBF kernel ($\sigma = 1$) predicts the received signal as GSM due to the Gaussian characteristics of Gaussian minimum shift keying (GMSK) used in the GSM waveform.

One should note that the proposed framework does not require a specific tensor processor such as graphics processing unit (GPU), as known that SVMs can run on the central processing unit (CPU) without serious degradation in performance. Moreover, the results show that SVM with SCF can perform high F_1–score even if it does not employ complex kernel. Thus, more complex kernel does not guarantee higher performance comparing to less complex kernel. In other words, SCF is a function which maps I/Q vectors to another space where the signals can be separated linearly. Also, the proposed system does not need a large dataset since

TABLE 3. Performance metrics of the SVM–based classifier with several kernels.

Kernel	Signal	**Precision**	**Recall**	F_1**–score**
Linear	WCDMA	0.94	1.00	0.97
	LTE	0.84	0.95	0.89
	GSM	1.00	0.82	0.90
	Average	0.93	0.92	0.92
Quadratic	WCDMA	0.58	1.00	0.73
	LTE	0.90	0.91	0.90
	GSM	0.94	0.25	0.39
	Average	0.81	0.72	0.68
Polynomial ($d = 3$)	WCDMA	0.78	1.00	0.87
	LTE	0.76	0.85	0.80
	GSM	1.00	0.59	0.74
	Average	0.84	0.81	0.81
MLP ($\kappa_1 = 1$, $\kappa_2 = -1$)	WCDMA	0.78	0.56	0.65
	LTE	0.54	0.84	0.66
	GSM	0.74	0.53	0.62
	Average	0.68	0.64	0.64
RBF ($\sigma = 1$)	WCDMA	0.00	0.00	0.00
	LTE	0.00	0.00	0.00
	GSM	0.33	1.00	0.50
	Average	0.11	0.33	0.17

it employs a basic (linear) kernel. Furthermore, the linear kernel is recommended to use when the number of feature is very high [43].

Above all, one should consider that the RBF kernel tends to be overfitted when comparing to the linear kernel. Let mathematically explain why the RBF kernel tends to be overfitted. Remembering (25), when a given test vector $\mathbf{x}^* = [x_1^*, x_2^*, \cdots, x_p^*]^T$ is far from (in terms of Euclidean distance) an observation $\mathbf{x}_k$ used in training, $|\mathbf{x} - \mathbf{x}_k|_2^2$ becomes large. Therefore, $\mathcal{K}(\mathbf{x}, \mathbf{x}_k)$ takes very small value, which corresponds to that training observations far from the test observation do not have an essential impact on the prediction [44]. As a result, the RBF kernel can be considered as overfitted. Thus, the complex kernels cannot fulfill high performance when the number of signal samples is kept constant. That is why the complex kernels cannot achieve high accuracy for our scenario and dataset.

C. THE NUMBER OF IN–PHASE AND QUADRATURE SAMPLES

The number of I/Q samples is an important parameter which affects the performance of the proposed algorithm. Therefore, the impacts of received samples on the classifier performance have been investigated by Monte–Carlo simulations. Table 4 presents the performance of the SVM classifier with respect to number of I/Q samples. As seen from Table 4, when the number of I/Q samples is less than 2048, the classification accuracy of the algorithm fluctuates due to insufficient samples to reveal the hidden periodicities within signals. GSM signals are recognized with high precision whatever the number of samples is because of the fact that GSM signals have a more basic structure compared to WCDMA and LTE. Therefore, a few samples for GSM allow observing the periodicities. According to Monte–Carlo simulations, the number of I/Q samples should be greater than 4096 to achieve a remarkable classification performance in SVMs.

TABLE 4. Performance metrics of the SVM–based classifier with respect to the number of received signal samples.

Number of Samples	Signal	**Precision**	**Recall**	F_1**–score**
64	WCDMA	0.65	0.64	0.64
	LTE	0.59	0.66	0.62
	GSM	0.98	0.85	0.91
	Average	0.74	0.72	0.73
128	WCDMA	0.66	0.66	0.66
	LTE	0.56	0.69	0.62
	GSM	0.98	0.77	0.86
	Average	0.74	0.71	0.71
256	WCDMA	0.66	0.70	0.68
	LTE	0.52	0.68	0.59
	GSM	0.97	0.62	0.76
	Average	0.72	0.67	0.68
512	WCDMA	0.68	0.83	0.75
	LTE	0.61	0.69	0.65
	GSM	0.99	0.66	0.79
	Average	0.76	0.73	0.73
1024	WCDMA	0.63	0.72	0.68
	LTE	0.57	0.66	0.61
	GSM	0.94	0.64	0.76
	Average	0.71	0.68	0.68
2048	WCDMA	0.65	0.77	0.71
	LTE	0.59	0.71	0.65
	GSM	0.91	0.57	0.70
	Average	0.72	0.68	0.68
4096	WCDMA	0.81	0.91	0.86
	LTE	0.79	0.81	0.80
	GSM	1.00	0.85	0.92
	Average	0.87	0.86	0.86
8192	WCDMA	0.90	0.98	0.94
	LTE	0.85	0.90	0.88
	GSM	1.00	0.86	0.92
	Average	0.92	0.91	0.91
16384	WCDMA	0.94	1.00	0.97
	LTE	0.84	0.95	0.89
	GSM	1.00	0.82	0.90
	Average	0.93	0.92	0.92

The proposed SVM model is tested by using the test dataset including signals which have not been observed by the model before. Therefore, these results show that the proposed system can be generalized, *i.e.* not overfitted.

D. PERFORMANCES VS. SIGNAL–TO–NOISE RATIO VALUES

In order to investigate the impact of SNR on the classification accuracy, the signal sets have been expanded to include the signals with SNR values ranging between 1 dB and 15 dB. The training set consists of 1000 signals for each class. The same procedure has been applied in order to construct the test set including 500 signals for each class at each SNR value.

The classification performance in regards to the different SNR values is shown in Table 5. Although it is expected that the classification performance gets better when SNR increases, the accuracy for GSM fluctuates due to the Gaussian low–pass filtering used in GSM signal generation. On the other hand, the performances for WCDMA and LTE are increasing as expected. The overall performance for three cellular communication signals is over 90% at 7 dB SNR. As a result, SCF produces reliable feature for the cellular communication signals in the environments with fading and multipath.

TABLE 5. Performance metrics with respect to SNR when the SCF is employed as feature vector in SVM for the signals with 16384 samples.

SNR	Signal	Precision	Recall	F_1–score
1dB	WCDMA	0.46	0.33	0.38
	LTE	0.47	0.34	0.39
	GSM	0.45	0.70	0.55
	Average	0.46	0.46	0.44
2dB	WCDMA	0.68	0.53	0.60
	LTE	0.53	0.40	0.46
	GSM	0.56	0.81	0.66
	Average	0.59	0.58	0.57
3dB	WCDMA	0.87	0.68	0.77
	LTE	0.69	0.58	0.63
	GSM	0.67	0.92	0.77
	Average	0.74	0.73	0.72
4dB	WCDMA	0.91	0.72	0.80
	LTE	0.75	0.74	0.74
	GSM	0.74	0.90	0.81
	Average	0.80	0.79	0.79
5dB	WCDMA	0.94	0.83	0.88
	LTE	0.78	0.88	0.83
	GSM	0.89	0.89	0.89
	Average	0.87	0.86	0.86
6dB	WCDMA	0.96	0.86	0.91
	LTE	0.77	0.94	0.85
	GSM	0.94	0.83	0.88
	Average	0.89	0.88	0.88
7dB	WCDMA	0.98	0.92	0.95
	LTE	0.81	0.97	0.89
	GSM	0.97	0.84	0.90
	Average	0.92	0.91	0.91
8dB	WCDMA	0.98	0.92	0.95
	LTE	0.81	0.97	0.89
	GSM	0.97	0.84	0.90
	Average	0.93	0.92	0.92
9dB	WCDMA	0.98	0.97	0.98
	LTE	0.78	0.98	0.87
	GSM	1.00	0.75	0.86
	Average	0.92	0.90	0.90
10dB	WCDMA	0.97	0.97	0.97
	LTE	0.82	0.97	0.89
	GSM	1.00	0.81	0.90
	Average	0.93	0.92	0.92
11dB	WCDMA	0.98	0.99	0.98
	LTE	0.82	0.97	0.89
	GSM	1.00	0.80	0.89
	Average	0.93	0.92	0.92
12dB	WCDMA	0.98	0.99	0.98
	LTE	0.87	0.98	0.92
	GSM	1.00	0.86	0.92
	Average	0.95	0.94	0.94
13dB	WCDMA	0.98	0.99	0.99
	LTE	0.90	0.98	0.94
	GSM	1.00	0.90	0.95
	Average	0.96	0.96	0.96
14dB	WCDMA	0.98	0.99	0.99
	LTE	0.93	0.98	0.96
	GSM	1.00	0.94	0.97
	Average	0.97	0.97	0.97
15dB	WCDMA	0.98	0.99	0.99
	LTE	0.95	0.98	0.97
	GSM	1.00	0.95	0.98
	Average	0.98	0.98	0.98

E. FADING

Our dataset includes real–world data; hence, there are many channel types in the dataset. The classification results show that the proposed system is robust to varying channel conditions. In order to observe the performance with respect to fading, we created a new dataset including signals generated

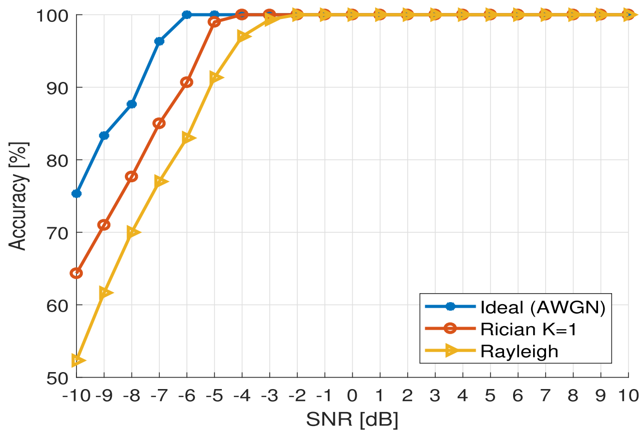

FIGURE 10. Classification performances of SVM and SCF with respect to ideal, Rician ($K = 1$) and Rayleigh channels.

in the simulation environment. Then, we used this dataset to observe the performance of the proposed model and SCF function with respect to the fading and SNRs. For each fading and SNR value, the training and test sets consist of 3000 and 1500 signals. In the simulation dataset, the number of three signal types is equal.

The simulation is performed for Ideal (AWGN only), Rician ($K = 1$), and Rayleigh fading channels with SNR values in between -10 dB and 10 dB. The multipath model is adopted from ITU–R M1225 Pedestrian B channel parameters detailed in [45]. The simulation results indicate that SCF and SVM show tremendous success in the classification of cellular communication signals as seen in Fig. 10. However, real–world conditions degrade the performance of the proposed classifier. For instance, the classifier achieves 90% accuracy when SNR is -5 dB for simulation dataset and 7 dB for real–world signal dataset, respectively. This result exhibits why we deal with signals received in real–world environments in this study since the real–world channels spoil the structure of the signals heavily because of Doppler shift, imperfections caused by electronic components and antennas, etc.

F. COMPARISON WITH EXISTING DEEP LEARNING NETWORKS

In order to observe how CLDNN and LSTM perform, we adopt the CLDNN [46] and LSTM [47] models which are used in modulation classification. We employ the same models and input vector and matrix as proposed in the papers. CLDNN employs a 2×128 matrix whose first and second rows include amplitude and phase values, respectively. Additionally, LSTM takes a vector with the length of 256, which created by concatenating 128 I and Q values, as an input. For all details, we refer the readers to [46], [47].

As given in Table 6, precision, recall, and F_1–score reveal poor performance of these classifier models for radio air interfaces. We also investigate LSTM network given in [47] with SCF instead of I/Q samples; however, the computation time is very high (i.e. 2 hour 29 minutes per epoch for the PC

TABLE 6. Performance metrics of the existing DL networks and the proposed system.

Model	Signal	**Precision**	**Recall**	F_1**–score**
CLDNN [48]	WCDMA	0.33	1.00	0.50
	LTE	0.00	0.00	0.00
	GSM	0.00	0.00	0.00
	Average	0.11	0.33	0.17
LSTM [49]	WCDMA	0.33	1.00	0.50
	LTE	0.00	0.00	0.00
	GSM	0.00	0.00	0.00
	Average	0.11	0.33	0.17
SVM with SCF	WCDMA	0.88	1.00	0.94
	LTE	1.00	0.87	0.93
	GSM	1.00	1.00	1.00
	Average	0.96	0.96	0.96

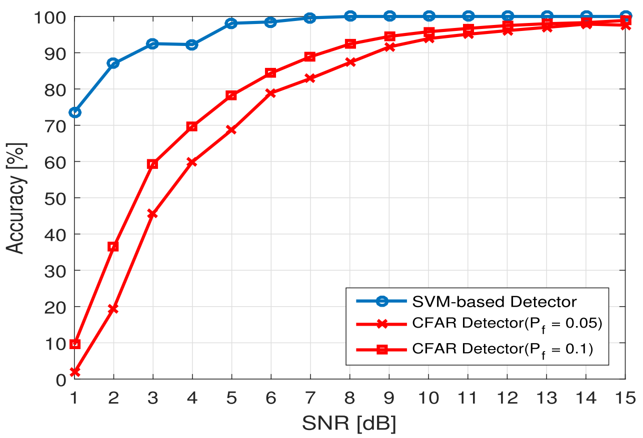

FIGURE 11. Spectrum sensing performances of SVM–based detector and CFAR detectors with respect to SNR.

with Nvidia GTX1070 Ti 11GB) since SCF outputs a vector with length of 16385. Thus, I/Q is employed in LSTM as given in [47] instead of SCF. On the other hand, even though LSTM takes 84 second for an epoch when I/Q samples are used as given in [47], using I/Q vector gives poor results.

G. SPECTRUM SENSING

The proposed SVM–based classifier is able to detect signals in the spectrum; hence, it can be employed in the cognitive radio networks. SVM–based detector employs SCF to differentiate signal from noise. SVM classifier is trained with 1200 signals (i.e. 600 noisy signals and 600 pure noise samples) for each SNR value. Then, the test process is carried out by using 800 signals (i.e. 400 noisy signals and 400 pure noise samples) for each SNR value. WCDMA signals are used since they have dominant SCF characteristics due to spreading codes. Also, CFAR detector which utilizes SCF, is employed to compare with SVM–based detector. Basically, CFAR detector includes a peak detector which searches the peaks of SCF with a constant false alarm rate. By searching peaks in the feature vector, the presence of the signal in the RF spectrum is determined. The false alarm rate comes from the peak detector in the CFAR detector. If the detector finds the peaks, the CFAR detector decides that a signal is present in the spectrum, otherwise not.

The real signals are employed in this study, also. The results show that SVM–based detector outperforms CFAR detector at low SNR values. For instance, the detection rate for SVM–based detector exceeds 92.5% at 3 dB SNR; however, CFAR detector senses the signals with detection rates of 45.6% and 59.4% when false alarm rates are 0.05 and 0.1, respectively. At high SNR values, SVM–based detector performs better compared to CFAR detector. Spectrum sensing performances with respect to SNR are depicted in Fig. 11 for SVM–based and CFAR detectors.

VII. CONCLUSION

Designing signal feature extractors and transforms to obtain the most suitable information to identify the wireless signals can pave the way towards more efficient and dynamic utilization of wireless RF spectrum. In this study, identification of wireless standard–based signals without any prior information by employing SCF, PSD, FFT and ACF under the umbrella of SVMs is proposed while considering many design parameters such as kernel type, number of I/Q samples and training input size.

SCF feature achieves the best performance for the identification of received signals in real–world wireless environments. Also, it is observed that other features are not robust against wireless channel conditions such as multipath fading and shadowing even though they have less computational complexity than SCF. This study shows that SVM with the linear kernel performs with an accuracy of 93%; however, other kernels cause SVM to have a poor performance. The effect of the number of I/Q samples on performance is also investigated. The accuracy fluctuates when the number of I/Q samples is less than 1024. The reason for this, I/Q sample number is not sufficient to extract features. It is seen that, after enough sample to extract statistics, there is proportion between success of classifier and sample number of received signal. Moreover, it is shown that the overall performance increases with SNR level. The overall accuracy reaches to 90% for the signal set with 7 dB SNR level and channel imperfections. It is shown that the features which are exploited within the proposed multi–dimensional signal identification framework can be used as a superior features to identify cellular communication signals in real–world conditions. Moreover, the proposed system achieves a high performance under a fading channel and low SNRs by using the dataset created in the simulation environment. Even if channel has Rayleigh fading, SVM performs a high accuracy at SNR as low as -3 dB.

It is observed that the proposed system achieves a significantly superior performance than the existing DL methods, which are commonly used in modulation classification. Additionally, this study shows that SVM together with SCF can be utilized in spectrum sensing with higher performance than conventional CFAR detector. Overall, SVM and SCF provide a convenient toolset for the classification of radio air interfaces as well as spectrum sensing.

TABLE 7. Abbreviations used in this study.

Abbreviation	Meaning
ACF	Auto-correlation Function
AM	Amplitude Modulation
AWGN	Additive white Gaussian Noise
CAF	Cyclic Auto-correlation Function
CDMA	Code Division Multiple Access
CFAR	Constant False Alarm Rate
CLDNN	Convolutional Long Short Term Memory Fully Connected Deep Neural Network
CNN	Convolutional Neural Network
CPU	Central Processing Unit
D2D	Device-to-Device
DL	Deep Learning
DVB	Digital Video Broadcasting
FAM	FFT Accumulation Method
FB	Feature Based
FCC	Federal Communications Commission
FFT	Fast Fourier Transform
FSK	Frequency Shift Keying
GMSK	Gaussian Minimum Shift Keying
GPU	Graphics Processing Unit
GSM	Global System for Mobile Communications
ISM	Industrial, Scientific and Medical
I/Q	In-phase/Quadrature
LB	Likelihood Based
LSTM	Long Short Term Memory
LTE	Long Term Evolution
MIMO	Multiple-input Multiple-output
MLP	Multi-layer Perceptron
OFDM	Orthogonal Frequency Division Multiplexing
PSD	Power Spectral Density
PSK	Phase Shift Keying
RBF	Radial Basis Function
RF	Radio Frequency
QAM	Quadrature Amplitude Modulation
QoS	Quality of Service
SCF	Spectral Correlation Function
SNR	Signal-to-Noise Ratio
SVM	Support Vector Machine
TETRA	Terrestrial Trunked Radio
t-SNE	t-distributed Stochastic Neighbor Embedding
WCDMA	Wideband Code Division Multiple Access
WFM	Wideband FM
WiMAX	Worldwide Interoperability for Microwave Access

As future work, a classifier model can be designed, which employs fewer I/Q samples without any deterioration in classification performance.

APPENDIX
GLOSSARY LIST

See Table 7.

REFERENCES

[1] X. Li, F. Dong, S. Zhang, and W. Guo, "A survey on deep learning techniques in wireless signal recognition," *Wireless Commun. Mobile Comput.*, vol. 2019, Feb. 2019, Art. no. 5629572.
[2] J. G. Andrews, S. Buzzi, W. Choi, S. V. Hanly, A. Lozano, A. C. Soong, and J. C. Zhang, "What will 5G be?" *IEEE J. Sel. Areas Commun.*, vol. 32, no. 6, pp. 1065–1082, Jun. 2014.
[3] F. Hameed, O. A. Dobre, and D. Popescu, "On the likelihood-based approach to modulation classification," *IEEE Trans. Wireless Commun.*, vol. 8, no. 12, pp. 5884–5892, Dec. 2009.
[4] P. Panagiotou, A. Anastasopoulos, and A. Polydoros, "Likelihood ratio tests for modulation classification," in *Proc. IEEE Military Commun. Conf. (MILCOM)*, vol. 2, Oct. 2000, pp. 670–674.
[5] J. L. Xu, W. Su, and M. Zhou, "Software-defined radio equipped with rapid modulation recognition," *IEEE Trans. Veh. Technol.*, vol. 59, no. 4, pp. 1659–1667, May 2010.
[6] A. K. Nandi and E. E. Azzouz, "Automatic analogue modulation recognition," *Signal Process.*, vol. 46, no. 2, pp. 211–222, 1995.
[7] S.-Z. Hsue and S. S. Soliman, "Automatic modulation recognition of digitally modulated signals," in *Proc. IEEE Mil. Commun. Conf. (MILCOM)*, Oct. 1989, pp. 645–649.
[8] K. C. Ho, W. Prokopiw, and Y. T. Chan, "Modulation identification by the wavelet transform," in *Proc. IEEE Mil. Commun. Conf. (MILCOM)*, vol. 2, Nov. 1995, pp. 886–890.
[9] L. Hong and K. C. Ho, "Identification of digital modulation types using the wavelet transform," in *Proc. IEEE Mil. Commun. Conf. (MILCOM)*, vol. 1, Nov. 1999, pp. 427–431.
[10] O. A. Dobre, Y. Bar-Ness, and W. Su, "Higher-order cyclic cumulants for high order modulation classification," in *Proc. Military Commun. Conf. (MILCOM)*, vol. 1, Oct. 2003, pp. 112–117.
[11] L. Liu and J. Xu, "A novel modulation classification method based on high order cumulants," in *Proc. Int. Conf. Wireless Commun., Netw. Mobile Comput. (WiCOM)*, Sep. 2006, pp. 1–5.
[12] A. Swami and B. M. Sadler, "Hierarchical digital modulation classification using cumulants," *IEEE Trans. Commun.*, vol. 48, no. 3, pp. 416–429, Mar. 2000.
[13] O. A. Dobre, "Signal identification for emerging intelligent radios: Classical problems and new challenges," *IEEE Instrum. Meas. Mag.*, vol. 18, no. 2, pp. 11–18, Apr. 2015.
[14] W. A. Gardner, "Exploitation of spectral redundancy in cyclostationary signals," *IEEE Signal Process. Mag.*, vol. 8, no. 2, pp. 14–36, Apr. 1991.
[15] R. S. Roberts, W. A. Brown, and H. H. Loomis, "Computationally efficient algorithms for cyclic spectral analysis," *IEEE Signal Process. Mag.*, vol. 8, no. 2, pp. 38–49, Apr. 1991.
[16] E. Karami, O. A. Dobre, and N. Adnani, "Identification of GSM and LTE signals using their second-order cyclostationarity," in *Proc. IEEE Int. Instrum. Meas. Technol. Conf. (I2MTC)*, May 2015, pp. 1108–1112.
[17] M. Oner and F. Jondral, "Cyclostationarity based air interface recognition for software radio systems," in *Proc. IEEE Radio Wireless Conf.*, Sep. 2004, pp. 263–266.
[18] M. Adrat, J. Leduc, S. Couturier, M. Antweiler, and H. Elders-Boll, "2nd order cyclostationarity of OFDM signals: Impact of pilot tones and cyclic prefix," in *Proc. IEEE Int. Conf. Commun. (ICC)*, Jun. 2009, pp. 1–5.
[19] A. A. Habashna, O. A. Dobre, R. Venkatesan, and D. C. Popescu, "Second-order cyclostationarity of mobile WiMAX and LTE OFDM signals and application to spectrum awareness in cognitive radio systems," *IEEE J. Sel. Topics Signal Process.*, vol. 6, no. 1, pp. 26–42, Feb. 2012.
[20] A. Fehske, J. Gaeddert, and J. H. Reed, "A new approach to signal classification using spectral correlation and neural networks," in *Proc. IEEE Int. Symp. New Frontiers Dyn. Spectr. Access Netw. (DySPAN)*, Nov. 2005, pp. 144–150.
[21] H. Hu, Y. Wang, and J. Song, "Signal classification based on spectral correlation analysis and SVM in cognitive radio," in *Proc. 22nd Int. Conf. Adv. Inf. Netw. Appl. (AINA)*, Mar. 2008, pp. 883–887.
[22] A. Selim, F. Paisana, J. A. Arokkiam, Y. Zhang, L. Doyle, and L. A. DaSilva, "Spectrum monitoring for radar bands using deep convolutional neural networks," in *Proc. IEEE Global Commun. Conf. (GLOBECOM)*, Dec. 2017, pp. 1–6.
[23] M. Schmidt, D. Block, and U. Meier, "Wireless interference identification with convolutional neural networks," in *Proc. IEEE 15th Int. Conf. Ind. Inform. (INDIN)*, Jul. 2017, pp. 180–185.
[24] M. Kulin, T. Kazaz, I. Moerman, and E. De Poorter, "End-to-end learning from spectrum data: A deep learning approach for wireless signal identification in spectrum monitoring applications," *IEEE Access*, vol. 6, pp. 18484–18501, 2018.
[25] S. Rajendran, W. Meert, D. Giustiniano, V. Lenders, and S. Pollin, "Deep learning models for wireless signal classification with distributed low-cost spectrum sensors," *IEEE Trans. Cogn. Commun. Netw.*, vol. 4, no. 3, pp. 433–445, Sep. 2018.
[26] M. Papadonikolakis and C.-S. Bouganis, "A novel FPGA-based SVM classifier," in *Proc. Int. Conf. Field-Program. Technol.*, Dec. 2010, pp. 283–286.
[27] C. Cardoso, A. R. Castro, and A. Klautau, "An efficient FPGA IP core for automatic modulation classification," *IEEE Embedded Syst. Lett.*, vol. 5, no. 3, pp. 42–45, Sep. 2013.
[28] Z. Wu, S. Zhou, Z. Yin, B. Ma, and Z. Yang, "Robust automatic modulation classification under varying noise conditions," *IEEE Access*, vol. 5, pp. 19733–19741, 2017.

[29] T. A. Almohamad, M. F. M. Salleh, M. N. Mahmud, and A. H. Y. Sa'D, "Simultaneous determination of modulation types and signal-to-noise ratios using feature-based approach," *IEEE Access*, vol. 6, pp. 9262–9271, 2018.

[30] H. Tayakout, I. Dayoub, K. Ghanem, and H. Bousbia-Salah, "Automatic modulation classification for D-STBC cooperative relaying networks," *IEEE Wireless Commun. Lett.*, vol. 7, no. 5, pp. 780–783, Oct. 2018.

[31] X. Lin, O. A. Dobre, T. M. N. Ngatched, Y. A. Eldemerdash, and C. Li, "Joint modulation classification and OSNR estimation enabled by support vector machine," *IEEE Photon. Technol. Lett.*, vol. 30, no. 24, pp. 2127–2130, Dec. 15, 2018.

[32] K. Tekbıyık, O. Akbunar, A. R. Ekti, G. Karabulut Kurt, and A. Görçin, "On the investigation of wireless signal identification using spectral correlation function and SVMs," in *Proc. IEEE Wireless Commun. Netw. Conf. (WCNC)*, Apr. 2019, pp. 1–5.

[33] K. Tekbıyık, O. Akbunar, A. R. Ekti, and A. Görçin, "Replication data for: Multi-dimensional wireless signal identification based on support vector machines," Tech. Rep., 2019. doi: 10.7910/DVN/BJBELX.

[34] C. S. Long, K. M. Chugg, and A. Polydoros, "Further results in likelihood classification of QAM signals," in *Proc. IEEE Mil. Commun. Conf.*, Oct. 1994, pp. 57–61.

[35] C. M. Spooner, "On the utility of sixth-order cyclic cumulants for RF signal classification," in *Proc. 35th Asilomar Conf. Signals, Syst. Comput.*, vol. 1, Nov. 2001, pp. 890–897.

[36] O. A. Dobre, Y. Bar-Ness, and W. Su, "Robust QAM modulation classification algorithm using cyclic cumulants," in *Proc. IEEE Wireless Commun. Netw. Conf.*, vol. 2, Mar. 2004, pp. 745–748.

[37] G. B. Giannakis, "Cyclostationary signal analysis," in *Digital Signal Processing Handbook*. New York, NY, USA: CRC Press, 1998, pp. 1–17.

[38] *Digital Cellular Telecommunications System (Phase 2+); Base Station System (BSS) Equipment Specification; Radio Aspects*, document 3GPP, TS 11.21 V8.11.0, Release 1999, Jun. 1999.

[39] A. Goldsmith, *Wireless Communications*. Cambridge, U.K.: Cambridge Univ. Press, 2005.

[40] J. A. Suykens, T. Van Gestel, and J. De Brabanter, *Least Squares Support Vector Machines*. Singapore: World Scientific, 2002.

[41] *Evolved Universal Terrestrial Radio Access (E–UTRA); User Equipment (UE) Radio Transmission and Reception*, document 3GPP, TS 36.101 V14.3.0, Apr. 2017.

[42] *Universal Mobile Telecommunications System (UMTS); Physical Layer—General Description*, document 3GPP, TS 25.201 V10.0.0, Release 10, Apr. 2011.

[43] C.-W. Hsu *et al.*, "A practical guide to support vector classification," Taipei, Taiwan, 2003. [Online]. Available: https://www.csie.ntu.edu.tw/~cjlin/papers/guide/guide.pdf

[44] G. James, D. Witten, T. Hastie, and R. Tibshirani, *An Introduction to Statistical Learning: With Applications in R*, vol. 112. New York, NY, USA: Springer, 2013.

[45] *Guidelines for Evaluation of Radio Transmission Technologies for IMT-2000*, document Rec. ITU-R M.1225, 1997. [Online]. Available: https://www.itu.int/dms_pubrec/itu-r/rec/m/R-REC-M.1225-0-199702-I!!PDF-E.pdf

[46] S. Ramjee, S. Ju, D. Yang, X. Liu, A. El Gamal, and Y. C. Eldar, "Fast deep learning for automatic modulation classification," 2019, *arXiv:1901.05850*. [Online]. Available: https://arxiv.org/abs/1901.05850

[47] S. Hu, Y. Pei, P. P. Liang, and Y.-C. Liang, "Robust modulation classification under uncertain noise condition using recurrent neural network," in *Proc. IEEE Global Commun. Conf. (GLOBECOM)*, Dec. 2018, pp. 1–7.

KÜRŞAT TEKBIYIK (S'19) received the B.Sc. degree (Hons.) in electronics and communication engineering from Istanbul Technical University, Istanbul, Turkey, in 2017, and the M.Sc. degree in telecommunication engineering from the Institute of Science, Istanbul Technical University, in 2019, where he is currently pursuing the Ph.D. degree. He was with Aselsan Inc., where he involved in system design of ground terminals for satellite communication. He is also with The Scientific and Technological Research Council of Turkey (TÜBİTAK), Informatics and Information Security Research Center (BİLGEM). He is the author of several publications and he worked in projects aiming secure communication. His research interests include algorithm design for signal intelligence, next-generation wireless communication systems, terahertz wireless communications, and machine learning.

ÖZKAN AKBUNAR received the B.Sc. degree from the Electrical and Electronics Engineering Department, Anadolu University, Eskişehir, Turkey. He is currently pursuing the M.Sc. degree with the Telecommunication Engineering Department, Istanbul Technical University, Istanbul, Turkey. He has been with The Scientific and Technological Research Council of Turkey, Informatics and Information Security Research Center, as a Research and Development Engineer, since December 2017. His main research areas are wireless communication systems, digital signal processing, machine learning, and radar.

ALİ RIZA EKTİ was born in Tarsus, Turkey. He received the B.Sc. degree in electrical and electronics engineering from Mersin University, Mersin, Turkey, in June 2006, the degree from the Universidad Politéchnica de Valéncia, Valencia, Spain, in 2005, the M.Sc. degree in electrical engineering from the University of South Florida, Tampa, Florida, in December 2009, and the Ph.D. degree in electrical engineering from the Department of Electrical Engineering and Computer Science, Texas A&M University, in August 2015. He is currently an Assistant Professor with the Electrical and Electronics Engineering Department, Balikesir University, and also a Senior Researcher with TUBITAK BILGEM. His current research interests include statistical signal processing, convex optimization, machine learning, resource allocation, and traffic offloading in wireless communications in 4G and 5G systems and smart grid design and optimization.

ALİ GÖRÇİN received the B.Sc. degree in electronics and telecommunications engineering, the master's degree in defense technologies from Istanbul Technical University, and the Ph.D. degree in wireless communications from the University of South Florida (USF), after working at Turkish Science Foundation (TUBITAK) on avionics projects for more than six years. He was with Anritsu Company, during his tenure in USF, and was with Reverb Networks and Viavi Solutions, after his graduation. He is currently holding an assistant professorship position with Yildiz Technical University, Istanbul, and also serving as the Vice President of the Informatics and Information Security Research Center of TUBITAK, responsible from testing and evaluation along with research and development activities on wireless communications technologies.

GÜNEŞ KARABULUT KURT received the B.S. degree (Hons.) in electronics and electrical engineering from Bogazici University, Istanbul, Turkey, in 2000, and the M.A.Sc. and Ph.D. degrees in electrical engineering from the University of Ottawa, Ottawa, ON, Canada, in 2002 and 2006, respectively. From 2000 to 2005, she was a Research Assistant with the CASP Group, University of Ottawa. From 2005 to 2006, she was with TenXc Wireless, where she was involved in location estimation and radio frequency identification systems. From 2006 to 2008, she was with Edgewater Computer Systems Inc., where she worked on high-bandwidth networking in aircraft and priority-based signaling methodologies. From 2008 to 2010, she was with Turkcell R&D Applied Research and Technology, Istanbul. Since 2010, she has been with Istanbul Technical University, where she is currently a Full Professor. She is the author of numerous publications and international patents. She was involved in various research projects, including STREP, EUREKA, and ITEA-2 projects on wireless networks. She served as a Management Committee Member of the COST Action 1104. She is a Marie Curie Fellow and her project REALMARS is selected to be a success story by the European Commission Research Executive Agency.

• • •